

## Supporting Information

for

# Aggregation-induced Preparation of Ultrastable Zinc Sulfide Colloidal Nanospheres and Their Photocatalytic Degradations of Multiple Organic Dyes

Wanting Yang, Xiaoli Liu, Dong Li, Louzhen Fan, and Yunchao Li\*

Department of Chemistry, Beijing Normal University, Beijing, 100875 (P. R. China)

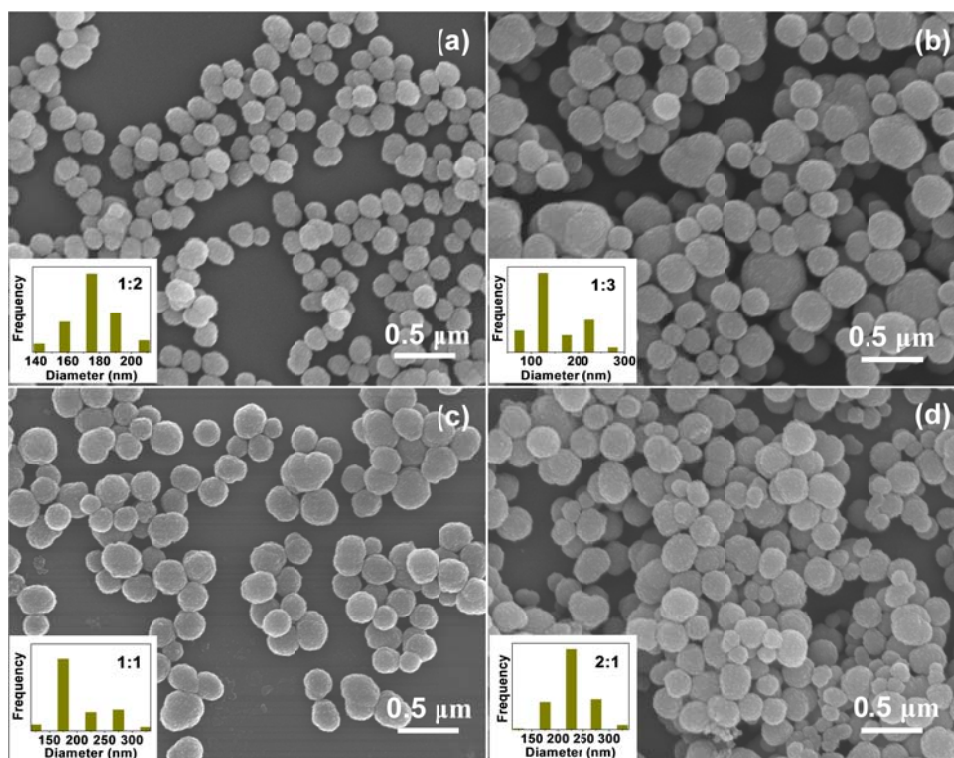


**Fig.S1** SEM images of the ZnS nanospheres prepared at different Zn/S ratio: (a) 1:2, (b) 1:3, (c) 1:1 and (d) 2:1. The Insets in (a) - (d) are their corresponding size distribution diagrams.

**Table S1** Sizes and size distribution of ZnS nanospheres synthesized at different experimental conditions.

Zn/S ratio	1:1	1:2	1:3	2:1	1:2			
$C_{Zn(O)_2}$ (g/mL)	0.052	0.052	0.035	0.103	0.031	0.036	0.042	0.052
Average Size(nm)	198	147	147	228	93	127	177	147
Standard deviation( $\delta$ )(%)	35	12	53	33	13	9	12	12

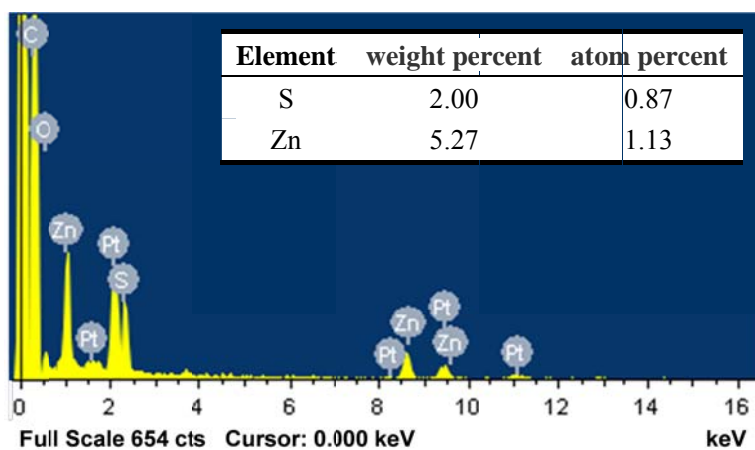


**Fig. S2** EDS spectrum of the ZnS nanospheres with a diameter of 147 nm.

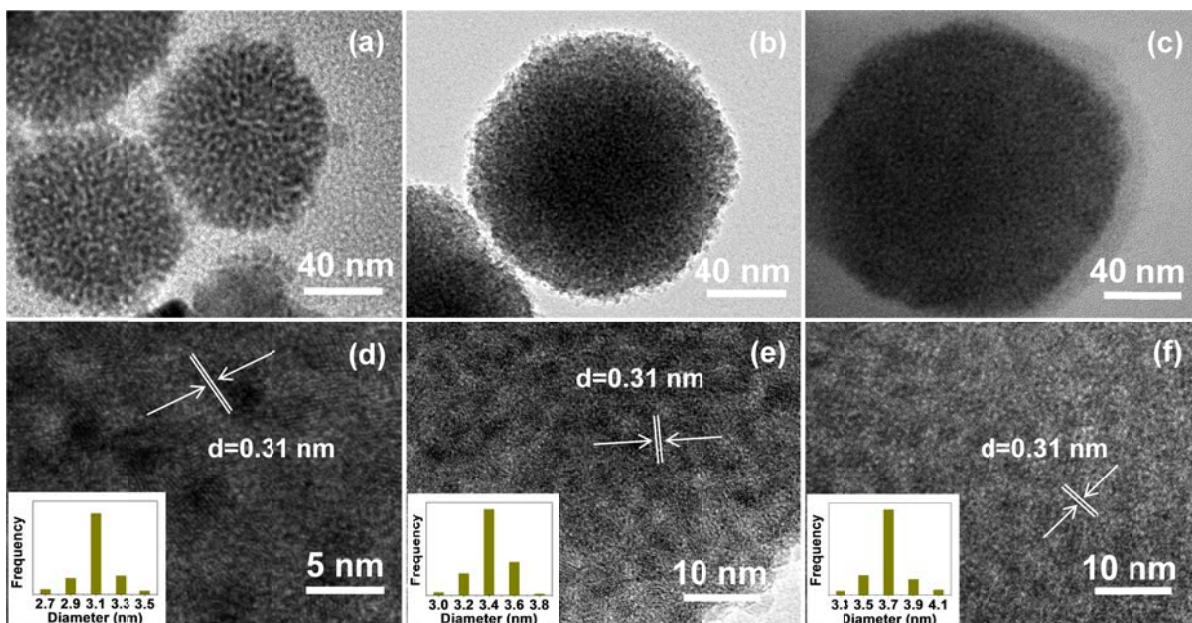


**Fig. S3** TEM images of ZnS nanospheres with different sizes: (a) 97 nm (b) 147 nm (c) 177 nm; (d), (e) and (f) are the HRTEM images corresponding to (a), (b) and (c) respectively. The insets are the size distribution diagrams of the nanoparticles consisting of such nanospheres.

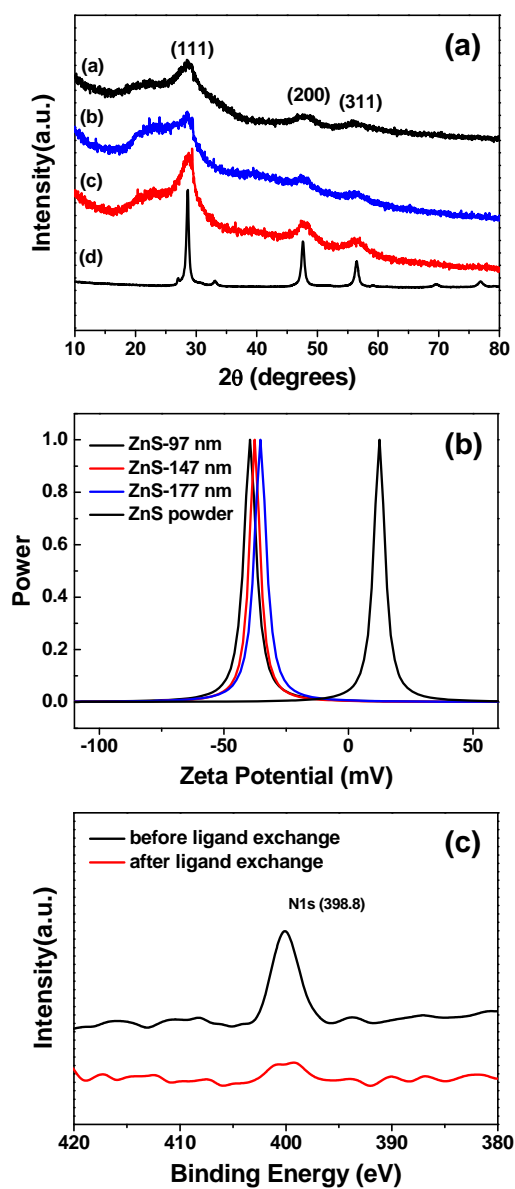


**Fig. S4** XRD patterns (a) and Zeta potentials (b) of the as-prepared ZnS nanospheres with different sizes. (c) XPS spectra of N<sub>1s</sub> core level from the ZnS nanospheres (177 nm) with (after) and without (before) ligand exchange.

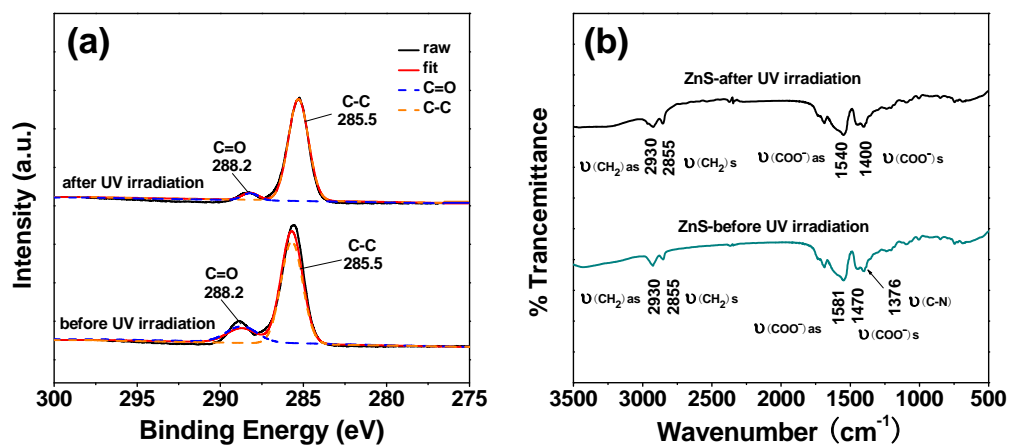


**Fig. S5** (a) XPS spectra of C<sub>1s</sub> and (b) FTIR spectra of the ZnS nanospheres (177 nm) with (after) and without (before) UV irradiation.

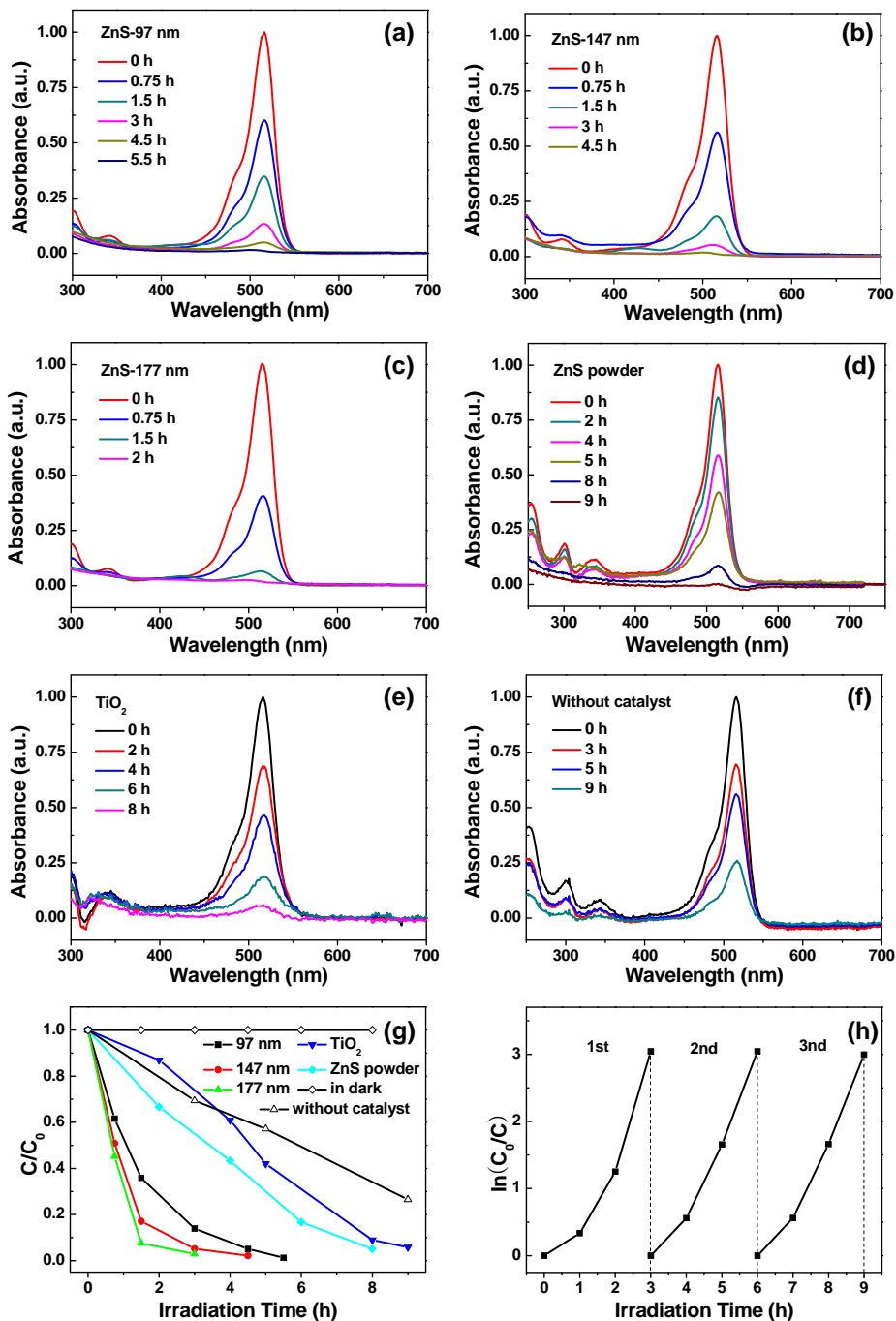


**Fig. S6** Temporal UV-visible absorption spectral observed for the solutions (10mL) containing  $5 \times 10^{-5}$  M eosin B in the presence of different catalysts (10 mg) as a function of irradiation time: (a) 97 nm ZnS NPs, (b) 147 nm ZnS NPs, (c) 177 nm NPs, (d) TiO<sub>2</sub> commercial powder, (e) ZnS commercial powder, and (f) without catalyst (self-degradation). (g) Time courses of dye concentration during photodegradation in the presence of different catalysts (C and C<sub>0</sub> are the actual concentration and initial concentration of eosin B respectively). (h) Recycling test on ZnS nanospheres for the photocatalytic degradation of EO solution under the UV light irradiation.

**Table S2** Carbon content of the eosin B and methylene blue solutions before and after photocatalytic degradation.

Dye	States	Carbon content in solution (mg/L)		
		Total Carbon (TC)	Total Inorganic Carbon (TIC)	Total Organic Carbon (TOC)
Eosin B ( $5 \times 10^{-5}$ M)	before degradation	11.23	0	11.23
	after degradation	10.91	10.54	0.37
Methylene blue ( $5 \times 10^{-5}$ M)	before degradation	9.422	0	9.422
	after degradation	8.549	8.295	0.254

**Table S3** Comparison of the photocatalytic performance of different catalysts toward the degradation of eosin B and methylene blue.

Catalyst	Dye	Experimental Conditions			Results			Ref
		Light Source	Dye/Catalyst	Stirring	Time /h	Efficiency %	Constants /h <sup>-1</sup>	
ZnS 97nm	EO MB				5.5 8		0.75 0.17	
ZnS 147nm	EO MB	125W Hg lamp (315-385nm)	3.1mg/100mg	Not Needed	4.5	100	0.86	This article
ZnS 177nm	EO MB				8		0.28	
ZnS powder	EO MB	125W Hg lamp (315-385nm)	3.1mg/100mg	continuous stirring	2	100	1.22	
TiO <sub>2</sub>	EO MB				7		0.62	
					9		0.27	
					>12		0.11	
					8		0.33	
					>12		0.17	
ZnS and CdS nanoparticles	MB	500W halogen lamp (400-800nm)	10.0mg/100mg	continuous stirring	6	63	0.21	Ref.S1
ZnSnano architectures	EO	125W mercury lamp (354nm)	9.4mg/100mg	continuous stirring	1	~100	----	Ref.S2
ZnS dravite	MB	100W Hg lamp (360nm)	0.13mg/100mg	continuous stirring	1	98	----	Ref.S3
CdS nanospheres	MB	300W Xe lamp ( $\geq 420$ nm)	4.4mg/100mg	continuous stirring	6	~100	----	Ref.S4

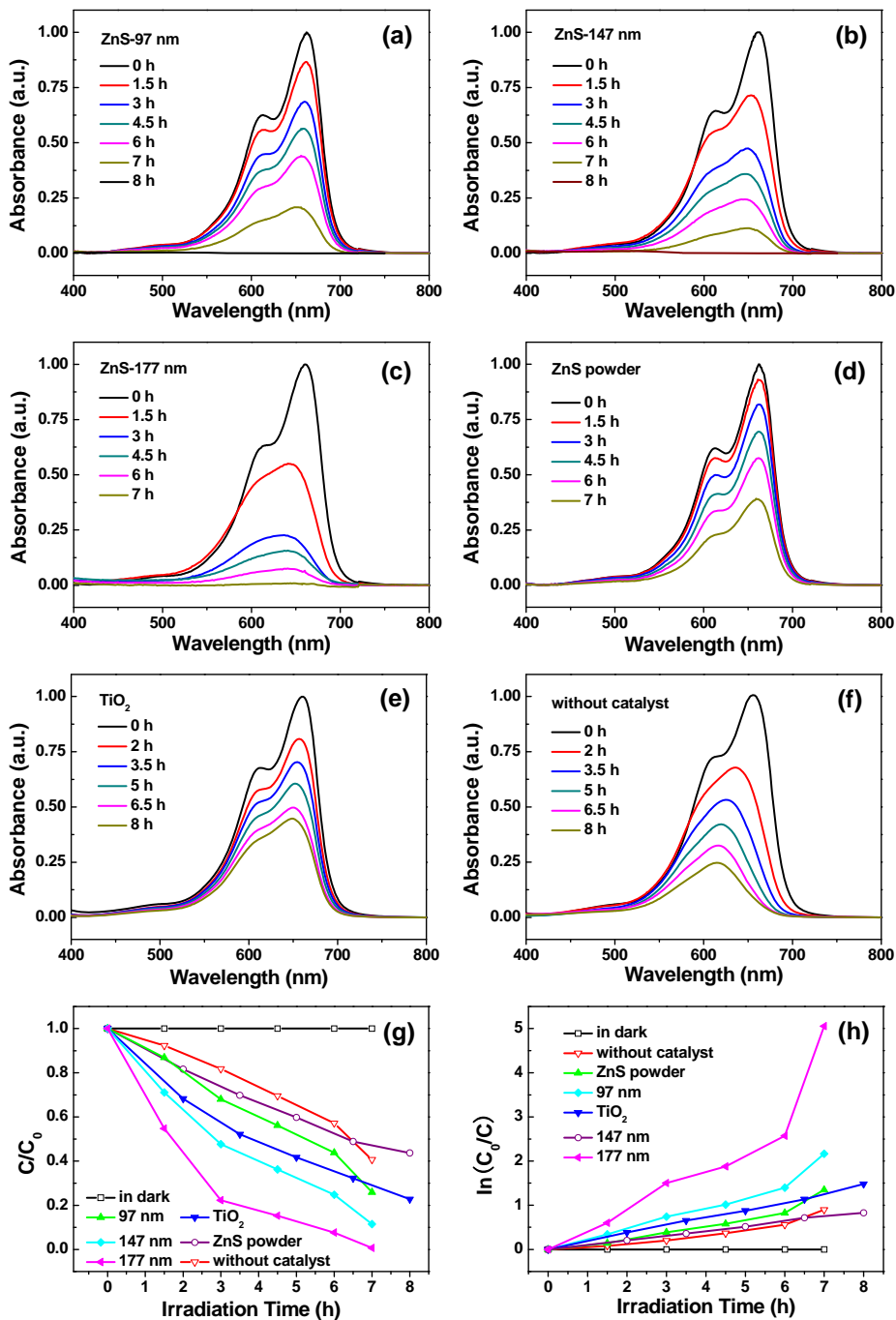


**Fig.S7** Temporal UV-visible absorption spectral observed for the solutions (10 mL) containing  $5 \times 10^{-5}$  M methylene blue in the presence of different catalysts (10 mg) as a function of irradiation time: (a) 97nm ZnS NPs, (b)147 nm ZnS NPs , (c) 177nm NPs, (d) ZnS commercial powder, (e) TiO<sub>2</sub> commercial powder and (f) without catalyst (self-degradation). (g) Time courses of dye concentration during photodegradation in the presence of different catalysts. (h) Plots of  $\ln(C_0/C)$  of methylene blue versus irradiation time, showing the fitting of the experimental data to the pseudo-first-order reaction model.



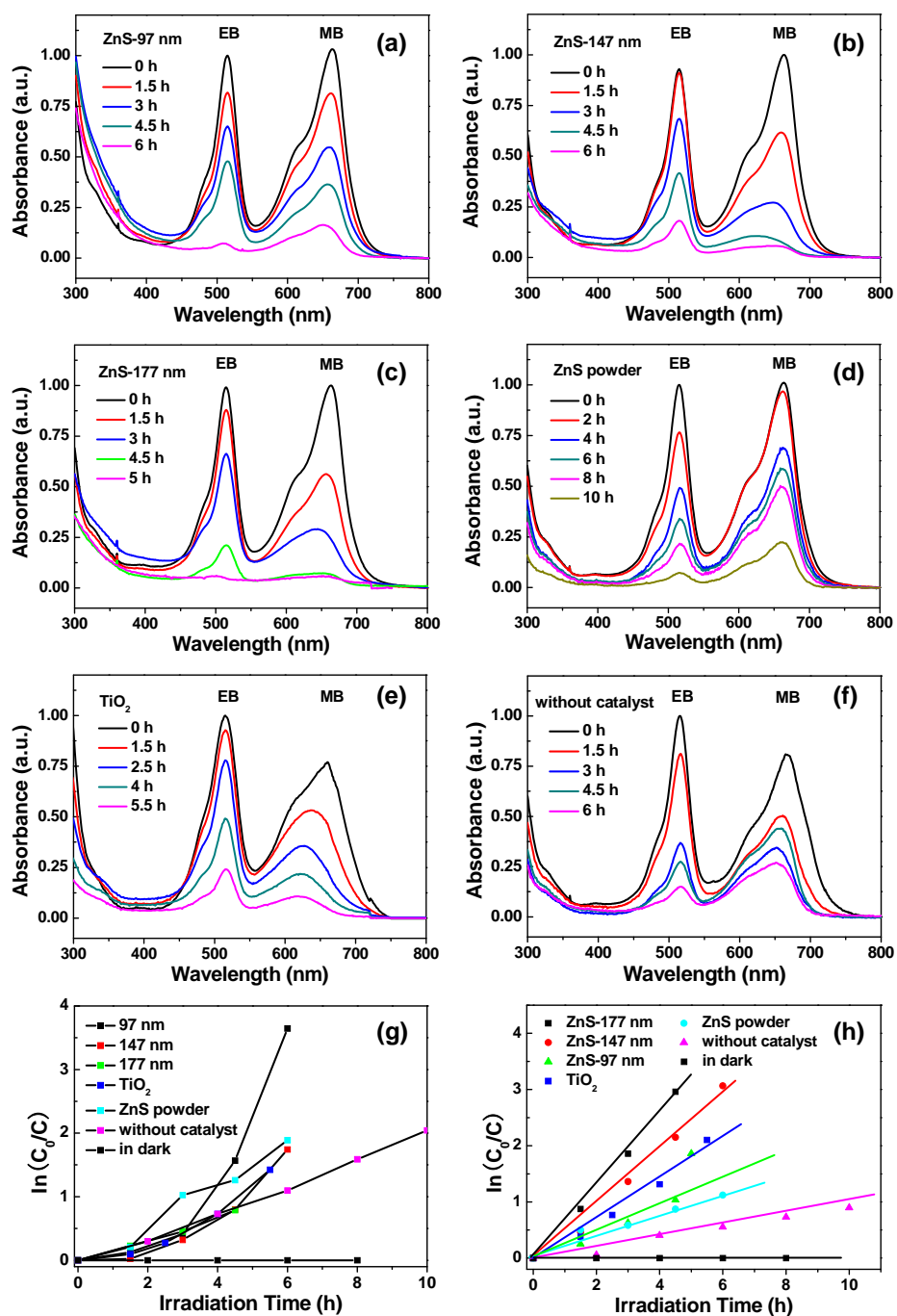


**Fig.S8** Temporal UV-visible absorption spectra observed for the methylene blue / eosin B binary system (MB :  $5 \times 10^{-5}$  M, EB :  $1 \times 10^{-4}$  M) in the presence of different catalysts as a function of illumination time: (a) 97 nm ZnS NPs, (b) 147 nm ZnS NPs, (c) 177 nm NPs, (d) ZnS commercial powder, (e) TiO<sub>2</sub> commercial powder and (f) without catalyst (self-degradation). Plots of  $\ln(C_0/C)$  of eosin B (g) and methylene blue (h) versus irradiation time, showing the fitting results with using the pseudo-first-order reaction model.

**Table S4** Photocatalytic performance of the as-prepared ZnS nanospheres toward the photodegradation of single dye and binary dye mixture under UV illumination.

Catalysts		ZnS-97nm		ZnS-147nm		ZnS-177nm		ZnS powder	
Dye		EO	MB	EO	MB	EO	MB	EO	MB
Reaction Constant /h <sup>-1</sup>	Single dye system	0.75	0.17	0.86	0.28	1.22	0.62	0.27	0.11
	Binary dye system	*	0.32	*	0.52	*	0.64	*	0.38

\*means the result does not obey the pseudo-first-order reaction model.

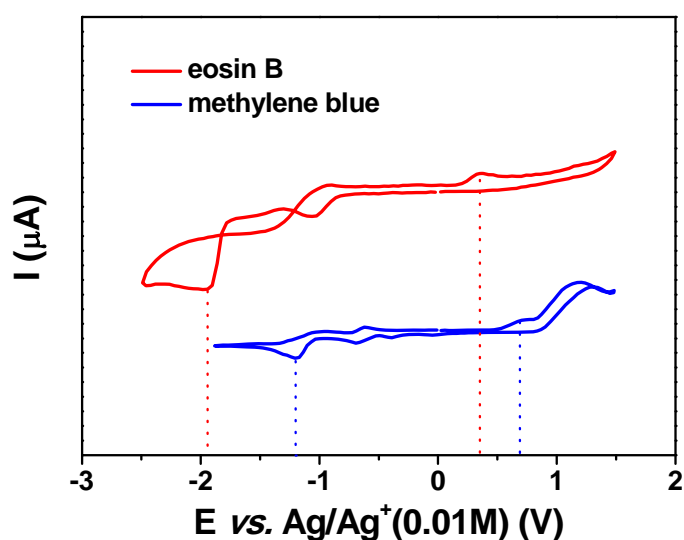


**Fig. S9** Cyclic voltammograms of eosin B (upper) and methylene blue (lower). Their HOMO and LUMO energy levels can be estimated from their oxidation peak potential and reduction peak potential respectively according to the protocol described in Ref. S5.

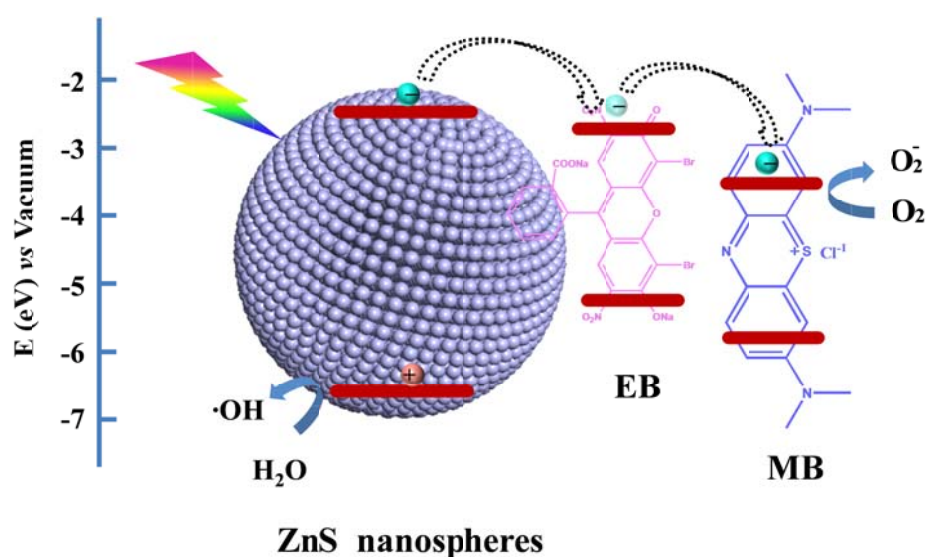


**Fig. S10** Schematic illustration of the alignment of the energy level of ZnS nanospheres, eosin and methylene blue and of electron transferring between them. The energy level of ZnS nanospheres, eosin and methylene blue are determined from their CV curves respectively; while the redox potential of  $E^0(\text{H}_2\text{O}/\cdot\text{OH})$  and  $E^0(\text{O}_2/\text{O}_2^{\cdot-})$  are referred to ref. S6

## References

- S1 N. Soltani, E. Saion, M. Z. Hussein, M. Erfani, A. Abedini, G. Bahmanrokh, M. Navasery and P. Vaziri, *Int. J. Mol. Sci.*, 2012, **13**, 12242-12258.
- S2 D. Chen, F. Huang, G. Ren, D. Li, M. Zheng, Y. Wang and Z. Lin, *Nanoscale*, 2010, **2**, 2062-2064.
- S3 J. H. Li, A. H. Lu, F. Liu and L. Z. Fan, *Solid State Ionics*, 2008, **179**, 1387-1390.
- S4 G. Lin, J. Zheng and R. Xu, *J. Phys. Chem. C*, 2008, **112**, 7363-7370.
- S5 a) C. Querner, P. Reiss, S. Sadki, M. Zagorska, A. Pron, *Phys. Chem. Chem. Phys.*, 2005, **7**, 3204; b) S. N. Inamdar, P. P. Ingole, S. K. Haram, *ChemPhysChem*, 2008, **9**, 2574
- S6 Fujishima, T. N. Rao and D. A. Tryk, *J. Photoch. Photobio.C.*, 2000, **1**, 1-21.